Geochemical Journal, Vol. 45, pp. 221 to 234, 2011

Dissolution processes of elements from subducting sediments into fluids: Evidence from the chemical composition of the Sanbagawa pelitic schists

SAEKO FUJIWARA, KOSHI YAMAMOTO* and KOICHI MIMURA

Graduate School of Environmental Studies, Nagoya University, Chikusa-ku, Nagoya 464-8601, Japan

(*Received March 26, 2010; Accepted January 14, 2011*)

In order to evaluate the dissolution processes of elements from subducting sediments into fluids during early stages of metamorphism (up to oligoclase–biotite zone at about 30 km depth), the chemical composition of Sanbagawa pelitic schists, Sanbagawa Metamorphic Belt, Japan was studied. Samples from different metamorphic grades show similarities in their major element and Rb compositions, suggesting that the Sanbagawa schists experienced insignificant dissolution of these elements. Arsenic, N (as ammonium, NH_4^+) and Cs contents decrease with increasing metamorphic grade, demonstrating that their dissolution is enhanced under respective metamorphic stages (As: upper–garnet zone, NH_4^+: chlorite ~ oligoclase–biotite zone, Cs: garnet ~ albite–biotite zone). Dissolution mechanisms proposed are as follows. The NH_4^+ dissolution accompanies dehydration of the pelitic schists, which may produce fluids with a high potential to dissolve or oxidize NH_4^+. The thermal structure of the subducted slab is likely to influence the depth of the NH_4^+ dissolution. The Cs dissolution is caused mainly by fluid flow from underlying meta-mafic rocks and the amount of fluids possibly controls the degree of the Cs dissolution. Heterogeneous dissolution of Cs suggests that the fluid flow from the underlying meta-mafic rocks has a channelized structure. The mechanism of As dissolution is not clearly understood; however, it may be strongly related to graphitization of kerogens in the pelitic schists. Differences in Cs dissolution were observed between the Sanbagawa pelitic schists and other well-studied meta-sedimentary sequences, particularly the Catalina Schist, California and New Caledonia Schistes Lustrés. In the case of the Catalina Schists, Cs was dissolved into fluids more effectively than the Sanbagawa pelitic schists. In contrast, meta-sedimentary rocks of the Schistes Lustrés nappe did not experience any Cs dissolution, although rocks subducted deeper than their dehydration depth. One of the reasons for these differences may be variations in the amount of channelized structures among subduction zones.

Keywords: element mobility, subduction zones, pelitic schists, fluid flow, graphitization

INTRODUCTION

Arc basalts are generally enriched in large-ion lithophile elements (LILE: Rb, Sr, Cs, Ba) plus As, Sb and Pb, and depleted in high field strength elements (HFSE: Nb, Zr, Ti) compared with MORB (Perfit *et al*., 1980; McCulloch and Gamble, 1991; Leeman, 1996). Some studies suggested that this chemical characteristic of arc basalts results from migration of fluids enriched in LILE and other elements from subducting slab to the mantle wedge. High-pressure experiments of Tatsumi *et al*. (1986), Kogiso *et al*. (1997) and Johnson and Plank (1999) demonstrated that LILE and LREE, which are enriched in arc basalts, can be more readily mobilized into fluids under *P-T* conditions experienced for subducted oceanic crust. Serpentinites exhumed from the mantle wedge are enriched in As, Sb and Pb (Hattori and Guillot, 2003) and brines from the top of Mariana forearc serpentine seamounts are also enriched in LILE and B (Mottl *et al*., 2004). These observations show that As, Sb, Pb, LILE and B can be mobilized during the early stage of prograde metamorphism up to eclogite facies. Other studies have indicated that subducting sediments are a major component from which the elements migrate to the mantle wedge (White and Dupré, 1985; Tera *et al*., 1986; Ben Othman *et al*., 1989; Plank and Langmuir, 1993). A comparison of chemical and/or isotopic compositions of arc basalts, MORB and marine sediments suggests that some components of subducting sediments are recycled to mantle wedge (e.g., Johnson and Plank, 1999). In contrast, Bebout (1995) and Spandler *et al*. (2003, 2004) proposed that LILE, Pb, LREE and B are not likely to be mobilized from subducting oceanic crust during the early stage of prograde metamorphism by up to amphibole facies (Bebout, 1995) and up to eclogite facies (Spandler *et al*., 2003, 2004).

These previous studies show that examination of element dissolution from subducting sediments into fluids during the early stage of prograde metamorphism is critically important for understanding element mobility in

*Corresponding author (e-mail: hamchans@nagoya-u.jp)

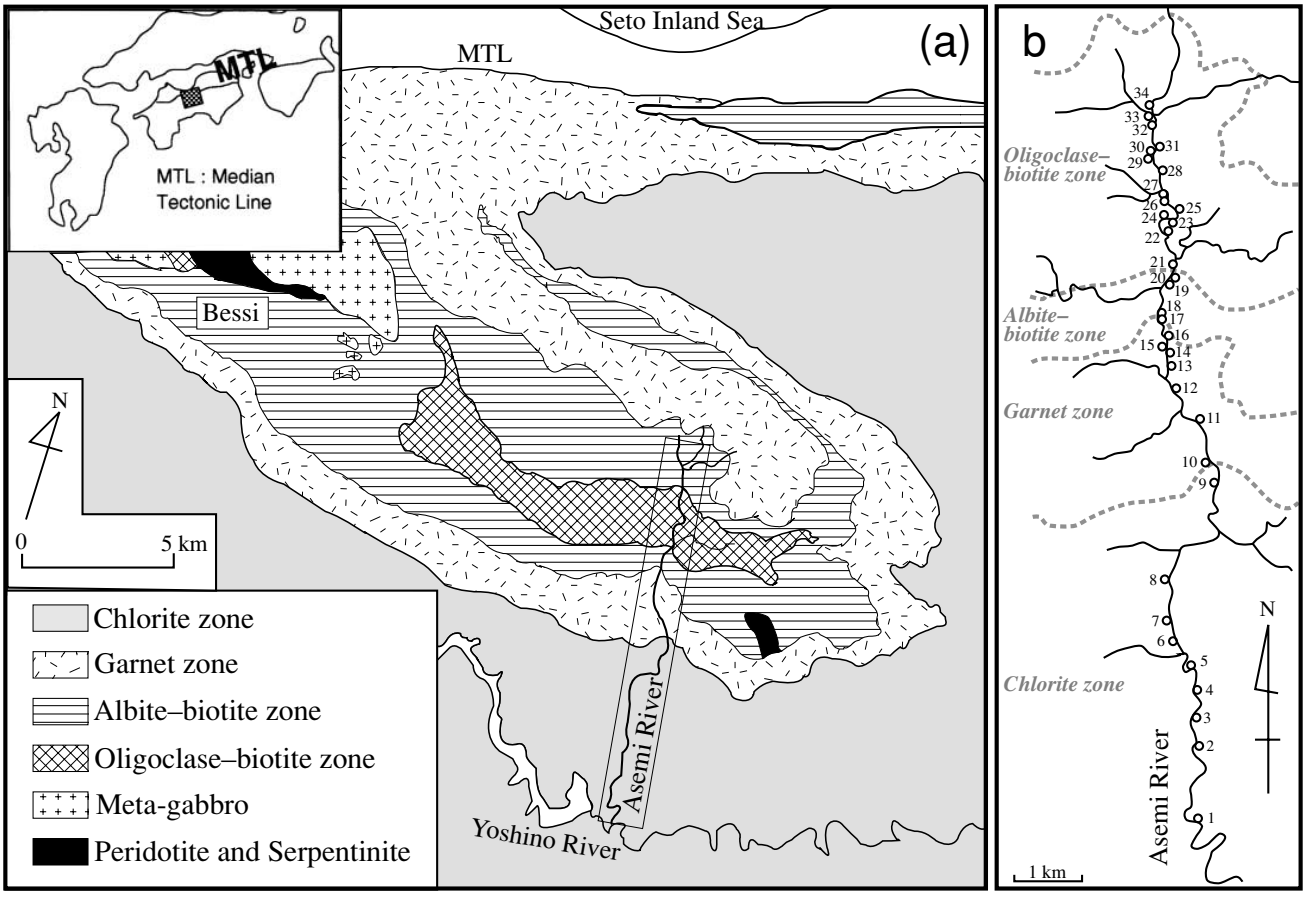

Fig. 1. (a) Metamorphic zone map of the Sanbagawa metamorphic belt in central Shikoku (modified from Higashino (1990) and Nakano and Nakamura (2001)). The sampling area is shown by the rectangular outline. (b) Sampling point along the Asemi River. Sample number is assigned in the order of increasing metamorphic grade.

subduction zones and element cycling in the Earth's interior.

Hydrothermal experiments were conducted to measure the chemical composition of fluids interacting with subducted decollement sediments. According to You *et al*. (1996), a hydrothermal system under low-*T*, low-*P* (80 MPa, 25~350°C) showed that equilibrated aqueous fluids had high Pb/Ce, Cs/Rb and B/Nb. This suggests that interaction between subducted sediments and fluids at shallow depth plays an important role in element migration from the slab to the mantle wedge. In contrast, an insignificant amount of dissolved elements (LILE, Pb etc.) into fluids was determined by a hydrothermal experiment under higher-*T*, higher-*P* conditions (2.2 GPa, 600~750°C; Spandler *et al*., 2007). This result clearly disagrees with that of You *et al*. (1996).

The element dissolution from subducting sediments into fluids has also been estimated by chemical analyses of exhumed meta-sedimentary rocks that experienced prograde metamorphism during subduction. In the case of the Catalina Schist, meta-sedimentary rocks exposed in California, Bebout *et al*. (1999) reported that samples which experienced prograde metamorphism under higher-*T* conditions (reaching up to epidote–blueschist/amphibolite or amphibolite facies) are depleted in N, B, Cs, As and Sb relative to the samples at lower-metamorphic grade (lawsonite–albite facies). This observation suggests that the dissolution of these elements from meta-sediments occurs in relatively warm subducting slabs during the early stage of prograde metamorphism. On the contrary, Spandler *et al*. (2003) examined samples of high-pressure, low-temperature metamorphic rocks from New Caledonia and concluded that significant amounts of trace elements are not liberated up to eclogite facies due to the decoupling of fluid release and trace element release in subducting slab. Thus, analyses of meta-sedimentary rocks can provide effective information for evaluation of the element dissolution from subducting sediments into fluids.

In this study, we analyzed the bulk chemical compo-

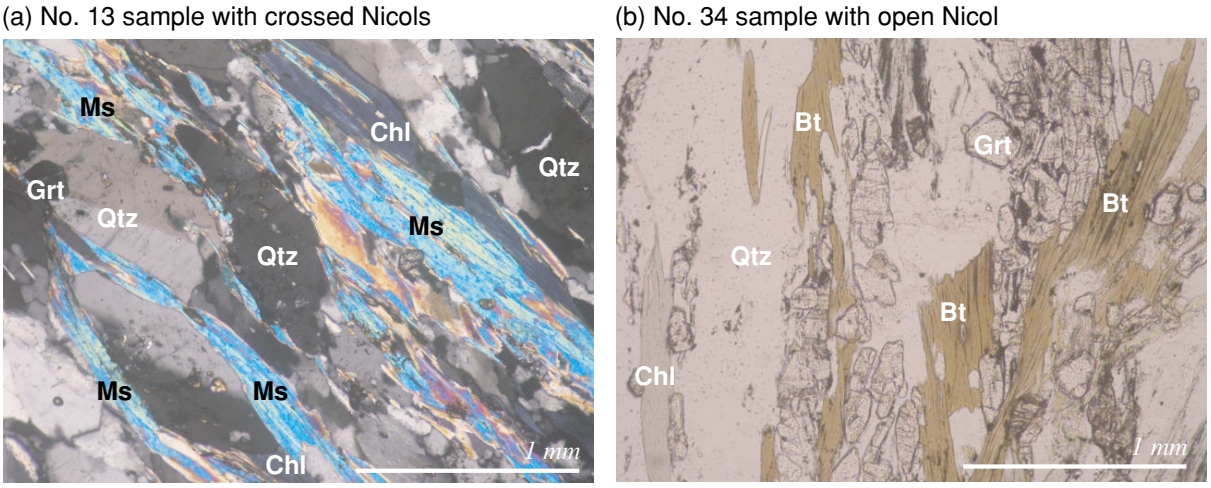

Fig. 2. Thin sections of the Sanbagawa pelitic schists. (a) A garnet zone sample (No. 13) and (b) an oligoclase–biotite zone sample (No. 34) (Bt = biotite, Chl = chlorite, Grt = garnet, Ms = muscovite, and Qtz = quartz).

sition of the Sanbagawa pelitic schists in order to identify (i) which elements were dissolved from the subducting sediments into fluids during metamorphism in the subduction zone and (ii) under which metamorphic stage the dissolution occurred. We further discuss the major factors controlling the element mobility into fluids and their variations among subduction zones.

Geological Background and Sample Description

The Sanbagawa metamorphic belt extends from eastern Japan (Kanto) to western (Kyushu) over a distance of about 800 km and is derived from an Early Cretaceous accretionary complex (Isozaki and Itaya, 1990; Wallis, 1998). The Sanbagawa belt is divided into non-eclogitic unit and eclogitic domains (Takasu, 1989; Wallis and Aoya, 2000).

The non-eclogite unit is composed largely of pelitic schists (meta-sedimentary rocks) and meta-mafic rocks and represents processes of underplating at depths of 15–30 km (Takasu, 1989). The pelitic schists in the non-eclogite unit belong to four metamorphic zones on the basis of their mineral assemblages: chlorite zone, garnet zone, albite–biotite zone and oligoclase–biotite zone in the order of increasing metamorphic grade (Banno *et al*., 1978; Enami, 1982). Peak *P-T* conditions range from 0.55 to 1.1 GPa and from 300 to 600°C, respectively (reviewed in Wallis *et al*., 2000), as estimated from Fe–Mg partitioning between chlorite and garnet (Banno and Sakai, 1989) and zonal structures of sodic pyroxene in equilibrium with albite and quartz (Enami *et al*., 1994).

We sampled pelitic schists along the Asemi River in central Shikoku (Fig. 1a), where lower to higher-grade metamorphic rocks are well exposed (Fig. 1b). In the sampling area the metamorphic grade increases from the chlorite to oligoclase–biotite zones from south to north. The metamorphic rocks along the Asemi River are mainly pelitic schists with minor amounts of psammitic and basic schists. Nine samples were collected in the chlorite zone, 8 samples in the garnet zone, 3 samples in the albite–biotite zone and 14 samples in the oligoclase–biotite zone (Fig. 1b).

All Sanbagawa pelitic schists analyzed in this study consist mainly of quartz, plagioclase and muscovite with a minor amount of opaque minerals, chlorite and epidote (Fig. 2a). The samples in the albite/oligoclase–biotite zone also contain garnet as a major component with a minor amount of biotite (Fig. 2b). A strong foliation is developed in all samples defined mainly by the preferred orientation of phengitic muscovite (Fig. 2a).

Analytical Methods

Rock samples were crushed and then milled down to 5 mm^3 using an iron mill. Sieving was used to separate fine particles of less than 124 μm to prevent some contamination of iron. After washed in an ultrasonic bath with 18.2 MΩ water, these samples were dried at 70°C for 1 day, and powdered into less than 124 μm with an agate ball mill.

A similar procedure was used to prepare samples for separation of kerogens, although washing in the ultrasonic bath was eliminated, and the samples were powdered to a size of less than 500 μm with a stainless steel ball mill.

Major element composition was analyzed by X-ray fluorescence (Shimadzu SXF-1200). The glass beads were prepared by fusing mixtures of powder samples and $Li_2B_4O_7$ in a weight ratio of 0.7:6.0. Sedimentary and

Table 1. (a) Analytical results of rock reference samples, JSl-1 and -2, issued by the Geological Survey of Japan (GSJ). Average values and RSD of each analyzed element are listed. Number means the number of repeated analyses. (b) Preferred contents and standard deviation cited from http://riodb02.ibase.aist.go.jp/geostand/welcomej.html

Sample	JSl-1			JSl-2		
	Average (ppm)	RSD (%)	Number	Average (ppm)	RSD (%)	Number
As	15.3	3.46	5	10.5	7.42	5
Rb	114	5.58	3	116	1.73	6
Cs	8.13	2.18	3	8.93	2.09	6

Sample	JSl-1		JSl-2	
	Preferred value (ppm)	Standard deviation (ppm)	Preferred value (ppm)	Standard deviation (ppm)
As	14.9	1.09	11.4	1.35
Rb	117	6.41	118	3.96
Cs	7.6	1.31	8.24	1.59

igneous rock reference samples issued by the Geological Survey of Japan (GSJ) were used for the calibration.

Trace element compositions (Rb, Cs and As) were analyzed by an inductively coupled plasma mass spectrometer (ICP-MS, Hewlett-Packard HP4500). About 30 mg of powder samples were digested using a mixture of HF and $HClO_4$, followed by evaporation on a hot plate. The digestion was repeated twice, and then only $HClO_4$ was added to the residue, followed by evaporation. After decomposition, the sample solutions dissolved in 2%-HNO_3 were centrifuged and the supernatant solutions were taken into a clean Teflon® beaker. The remnants were decomposed by mixture of HF and $HClO_4$ and then centrifuged in the same way. The supernatants were added to the Teflon® beaker. This treatment was repeated until almost no remnants were found. The supernatant solutions were dried up and dissolved in 2%-HNO_3. The standard solutions were prepared by diluting and mixing commercial 1000 ppm solutions (Kishida Chemicals, Chameleon Reagents for Atomic Absorption Analysis). The internal standard solution, 200 ppb In, was also used for analyses. In the case of As analysis, $^{40}Ar^{35}Cl$ interferes with ^{75}As. The corrected ^{75}As signal was estimated by using the following equation:

$$^{75}\text{As signal} = [m/z\ 75\ \text{signal}] - 3.127([m/z\ 77\ \text{signal}] - 0.815\ [m/z\ 82\ \text{signal}]). \quad (1)$$

This equation means that (i) ^{77}Se is estimated on the basis of natural abundance ratio of $^{77}Se/^{82}Se = 0.815$; (ii) $^{40}Ar^{37}Cl$ is calculated by the subtraction of ^{77}Se from the total 77 signal; (iii) $^{40}Ar^{35}Cl$ is estimated on the basis of $^{40}Ar^{35}Cl/^{40}Ar^{37}Cl = 3.127$ (natural abundance ratio of $^{35}Cl/^{37}Cl$); and finally (iv) ^{75}As is calculated by subtraction of $^{40}Ar^{35}Cl$ from the total 75 signal.

We tested the reliability of the trace element (Rb, Cs and As) analyses, rock reference samples, JSl-1 and JSl-2, issued by GSJ were used for comparison. Each measured element is within the given content $\pm 1\sigma$ (Table 1). Relative standard deviations (RSD) of the analytical errors are low enough for the following discussions.

Organic element compositions (C, H and N) were determined by a EuroVector® CHNS-O Elemental Analyzer. About 20 mg of powder samples were wrapped in tin capsules. We used L-cystine ($C_6H_{12}N_2O_4S_2$) or 2,5-Bis(5-tert-butyl-2-benzoxazolyl) thiophene (hereafter BBOT; $C_{26}H_{26}N_2O_2S$) for the standard samples.

For the gravimetric determinations of H_2O (–) and loss on ignition (LOI), quartz tubes containing about 300 mg of powder samples were heated at 110°C for 2~3 hours and at 900°C for 1~2 hours, respectively.

The C, H, N and O contents in separated kerogens were determined as follows. Powder samples of about 100 g were decomposed by repeated treatment with HCl and HF. Between repeated acid treatments, the solutions were removed and the remnants were washed with distilled water twice. The remnants were treated by bromoform flotation in order to remove heavy minerals such as pyrite and zircon. Then low molecular weight organic compounds were also removed by Soxhlet extraction with chloroform for 3 days. We regarded the remnants obtained by these procedures as "kerogens".

The organic elements (C, H, N and O) of the kerogens were analyzed with a EuroVector® CHNS-O Elemental Analyzer. About 1 mg of kerogen was wrapped in a tin or silver capsule for the analysis of C, H, N or O, respec-

Table 2. Major and trace element compositions of the Sanbagawa pelitic schists

No.	1	2	3	4	5	6	7	8	9	10	11	12	13	14	15	16	17
Zone	Chlorite Zone									Garnet Zone							
SiO_2 (wt%)	64.80	70.40	62.17	71.81	58.33	60.68	68.35	67.65	63.69	66.19	68.95	75.13	71.64	72.37	69.25	56.23	64.65
TiO_2	0.595	0.439	0.558	0.405	0.802	0.723	0.629	0.516	0.656	0.637	0.524	0.335	0.401	0.411	0.480	0.457	0.650
Al_2O_3	16.44	14.16	15.14	14.10	19.50	17.52	14.69	13.93	17.16	15.95	14.18	12.28	13.08	12.84	13.65	10.95	14.31
Fe_2O_3*	5.86	3.19	4.43	3.17	6.33	6.28	4.56	5.16	5.37	4.22	4.53	2.64	2.79	3.33	4.95	5.36	5.82
MnO	0.250	0.048	0.122	0.067	0.114	0.080	0.057	0.188	0.155	0.093	0.225	0.047	0.052	0.066	0.265	0.292	0.216
MgO	2.10	1.20	1.67	1.21	2.32	2.48	1.73	1.89	1.96	1.66	1.74	0.96	0.95	1.12	1.77	6.56	2.32
CaO	0.048	1.17	7.34	0.44	0.65	0.68	0.86	0.93	0.61	0.57	0.54	0.46	0.85	1.55	0.68	6.98	1.58
Na_2O	2.10	4.88	1.23	4.19	2.25	2.44	2.86	2.17	3.71	2.66	2.34	2.56	4.04	3.01	1.70	1.22	2.12
K_2O	3.24	1.57	1.59	1.86	4.14	3.24	2.68	2.60	2.87	3.27	2.79	2.50	2.00	2.49	3.02	1.46	3.05
P_2O_5	0.086	0.095	0.089	0.085	0.126	0.136	0.103	0.093	0.102	0.094	0.067	0.050	0.052	0.065	0.074	0.079	0.100
$H_2O(+)$	4.29	2.02	3.45	2.10	3.91	3.75	2.61	3.15	4.27	2.80	3.50	2.32	2.02	1.66	2.56	4.31	2.63
$H_2O(-)$	0.47	0.16	0.28	0.04	0.31	0.39	0.33	0.32	0.54	0.46	0.55	0.18	0.60	0.031	0.12	0.11	0.08
Total (1)	100.28	99.33	98.05	99.48	98.79	98.39	99.45	98.60	101.10	98.61	99.94	99.45	98.48	98.94	98.52	94.01	97.53
LOI	4.15	2.33	4.19	1.86	4.56	4.53	3.44	3.84	4.59	3.41	3.80	2.55	2.97	2.16	2.53	8.94	3.25
Total (2)	99.67	99.48	98.52	99.20	99.13	98.77	99.95	98.97	100.87	98.75	99.70	99.50	98.82	99.41	98.38	98.53	98.07
As (ppm)	8.59	2.35	7.65	2.66	9.96	7.80	7.74	6.86	6.70	9.96	4.94	n.d.	n.d.	2.46	n.d.	2.17	n.d.
Rb	132	59	54	75	162	127	97	109	121	140	114	101	84	93	130	58	114
Cs	9.16	2.81	2.83	3.87	9.77	7.41	4.81	6.51	7.62	8.22	6.46	5.89	5.09	6.03	7.78	2.89	6.83
N (wt%)	0.049	0.025	0.020	0.025	0.078	0.068	0.039	0.068	0.042	0.048	0.041	0.034	0.026	0.027	0.033	0.016	0.030
C	0.33	0.20	0.79	0.15	0.90	1.04	0.68	0.61	0.52	0.36	0.29	0.37	0.19	0.51	0.31	1.64	0.58
H	0.53	0.24	0.41	0.24	0.47	0.46	0.33	0.39	0.54	0.36	0.45	0.28	0.29	0.19	0.30	0.49	0.30

No.	18	19	20	21	22	23	24	25	26	27	28	29	30	31	32	33	34
Zone	Albite–biotite Zone			Oligoclase–biotite Zone													
SiO_2 (wt%)	70.84	62.75	68.43	65.92	68.40	69.02	66.01	68.77	66.98	66.66	66.18	73.41	72.94	70.89	60.68	66.37	72.60
TiO_2	0.521	0.582	0.570	0.625	0.583	0.586	0.606	0.511	0.578	0.597	0.554	0.495	0.441	0.454	0.727	0.608	0.340
Al_2O_3	13.91	16.31	14.50	15.62	14.88	14.92	14.99	13.52	14.96	15.02	14.99	12.77	12.22	13.52	17.46	14.65	13.26
Fe_2O_3*	4.63	6.12	4.84	6.00	5.58	5.66	5.93	4.19	5.00	5.26	5.08	3.82	3.80	3.45	5.77	5.60	2.86
MnO	0.142	0.195	0.307	0.373	0.271	0.269	0.338	0.131	0.152	0.185	0.197	0.049	0.071	0.081	0.195	0.161	0.082
MgO	1.77	2.37	2.43	1.95	2.08	2.01	1.79	1.50	1.82	1.70	1.85	1.42	1.16	1.25	1.97	2.19	0.80
CaO	0.66	1.18	0.94	1.29	1.06	1.13	1.04	2.35	1.98	1.60	1.68	1.28	1.42	2.06	1.72	1.56	2.00
Na_2O	1.69	2.25	2.60	2.71	1.70	1.55	2.29	2.56	2.34	2.50	1.62	2.23	1.72	3.66	4.21	1.51	3.58
K_2O	3.26	3.29	2.49	2.88	3.05	3.07	2.68	2.42	3.00	2.81	3.34	2.43	2.52	1.88	2.52	3.72	2.71
P_2O_5	0.082	0.080	0.101	0.095	0.100	0.087	0.092	0.092	0.082	0.084	0.092	0.095	0.070	0.082	0.081	0.101	0.049
$H_2O(+)$	3.06	3.13	2.67	2.92	2.67	2.44	2.25	1.45	2.66	1.68	2.32	1.91	1.65	1.48	2.36	2.28	1.71
$H_2O(-)$	0.26	0.09	0.33	0.23	0.23	0.17	0.06	0.09	0.45	0.14	0.03	0.18	0.08	0.26	0.05	0.22	0.28
Total (1)	100.81	98.33	100.21	100.61	100.59	100.91	98.08	97.58	99.99	98.22	97.94	100.08	98.09	99.08	97.74	98.96	100.26
LOI	2.89	3.19	2.84	3.34	2.77	2.54	2.21	2.26	4.03	1.94	2.47	2.42	2.15	2.91	3.08	2.50	2.60
Total (2)	100.38	98.31	100.06	100.81	100.46	100.85	97.98	98.31	100.92	98.35	98.06	100.41	98.51	100.25	98.41	98.97	100.87
As (ppm)	n.d.	n.d.	n.d.	n.d.	n.d.	n.d.	n.d.	n.d.	n.d.	n.d.	n.d.	n.d.	n.d.	n.d.	n.d.	n.d.	n.d.
Rb	139	134	102	116	127	122	114	98	109	125	93	94	94	66	101	111	97
Cs	4.75	6.00	4.28	7.12	6.35	5.62	7.63	5.29	6.50	5.44	5.31	3.93	3.76	2.96	5.70	4.43	5.21
N (wt%)	0.033	0.037	0.035	0.038	0.033	0.036	0.030	0.019	0.024	0.021	0.026	0.033	0.025	0.021	0.029	0.026	0.016
C	0.11	0.55	0.28	0.50	0.26	0.25	0.33	0.57	0.54	0.41	0.44	0.59	0.42	0.71	0.94	0.41	0.26
H	0.37	0.36	0.33	0.35	0.32	0.29	0.26	0.17	0.35	0.20	0.26	0.23	0.19	0.19	0.27	0.28	0.22

Note: Fe_2O_3 denotes total iron as Fe_2O_3 and LOI does loss on ignition. Total (1) means the total contents of major elements, H_2O (+) and H_2O (−). Total (2) means the total of major elements and LOI.*

"n.d." means not detected because of under detection limit.

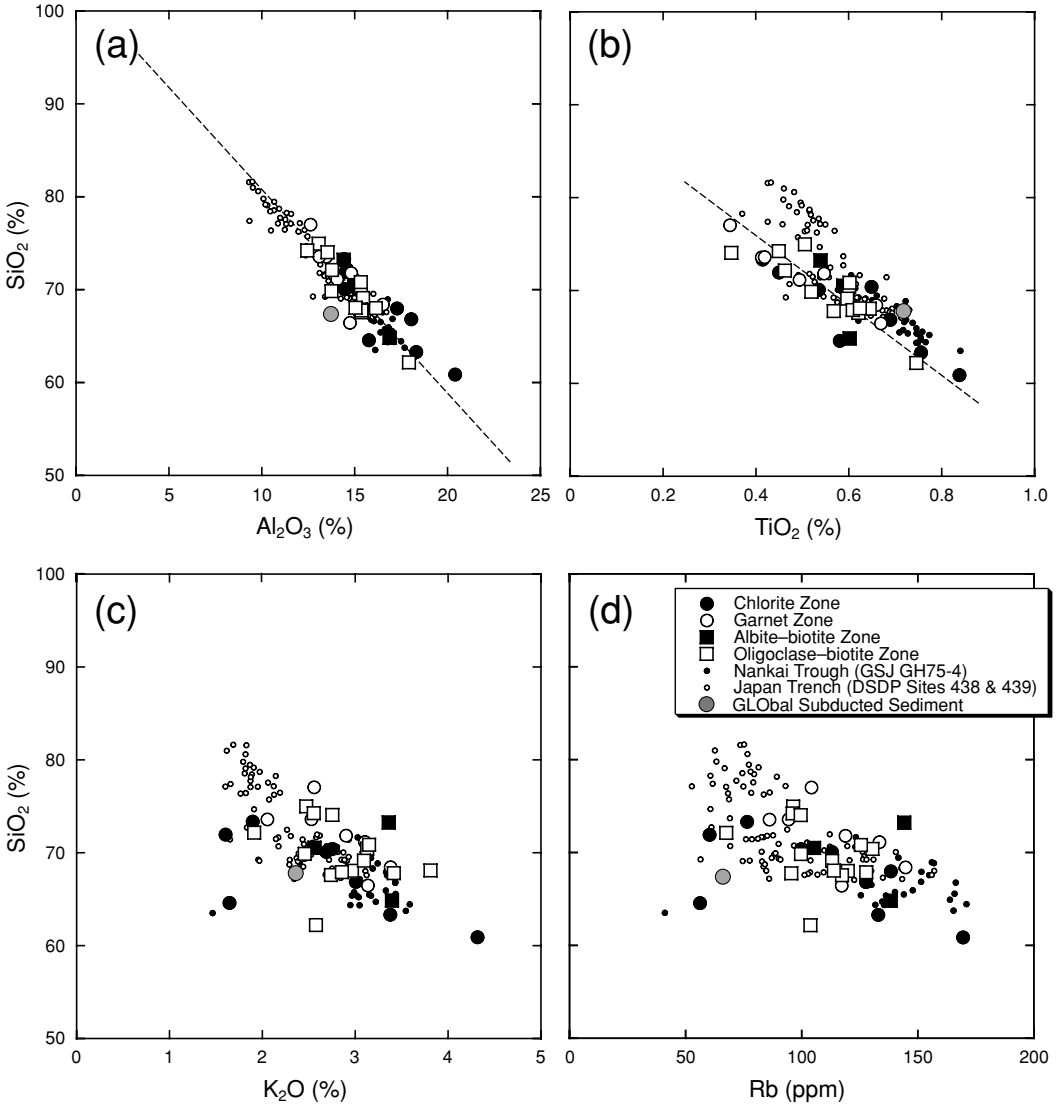

Fig. 3. Major element compositions of the Sanbagawa pelitic schists and marine sediments; relationship diagrams of (a) Al_2O_3, (b) TiO_2, (c) K_2O and (d) Rb against SiO_2. Large symbols represent the Sanbagawa pelitic schists from respective metamorphic zones. One Garnet zone sample (sample No. 16) with significant amounts of Ca carbonate is excluded. Small symbols represent chemical compositions of marine sediments cored at Japan Trench (Sugisaki, 1981) and Nankai Trough (Sugisaki, 1978) along Japan Arc. Large gray circle represents GLOSS (global subducted sediment) composition by Plank and Langmuir (1998). Every value is recalculated on water and other volatiles free basis.

tively. Standard was BBOT or acetanilide (C_8H_9NO) for the analysis of C, H, N or O, respectively. The degree of graphitization was also determined with an X-ray diffractometer (Rigaku-Denki, MultiFlex) using indices of apparent d_{002} and peak width.

Results and Discussion

Analytical results are presented in Table 2. In the following discussion, re-calculated compositions on a volatile free basis and elemental ratios are used to eliminate the contribution of volatile components such as H_2O.

All analyzed Sanbagawa samples of any metamorphic grade show little variations in their conservative element (Si, Ti, Al, K and Rb) composition. Major element and Rb compositions correspond to those of their source material, i.e., marine sediments (Fig. 3). This result suggests that these elements did not undergo significant dissolution into fluids during prograde metamorphism.

Figures 3a and 3b show clear negative correlations between SiO_2, Al_2O_3 and TiO_2, all data points overlapping irrespective of the sample metamorphic grade. Such

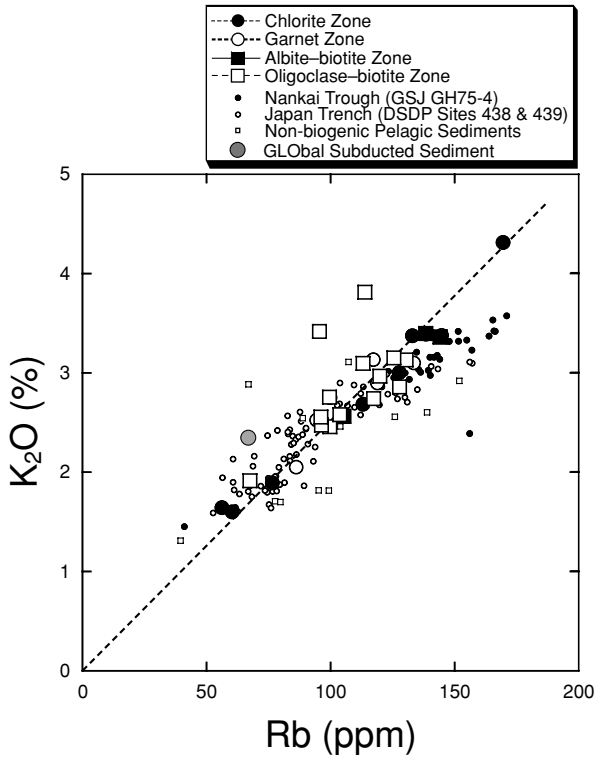

Fig. 4. Relationship diagram between K_2O with Rb in Sanbagawa pelitic schists. Sample symbols are the same as those in Fig. 3. Non-biogenic marine sediments from world-wide ocean was also plotted by small open squares (Ben Othman et al., 1989). Large gray circle represents GLOSS (global subducted sediment) composition by Plank and Langmuir (1998).

a characteristic is common to marine sediments along Japan Arc such as the Japan Trench and the Nankai Trough. This relationship is attributed to clastic detritus being diluted by the contribution of biogenic silica (Sugisaki, 1981), Ti and Al neither precipitating nor being dissolved during weathering and sedimentation (Sugisaki and Yamamoto, 1984). The SiO_2 contents of all Sanbagawa samples are comparable to those of marine sediments and show no systematic change with increasing metamorphic grade. For these reasons, SiO_2, TiO_2 and Al_2O_3 compositions of all samples are interpreted to be mostly inherited from their source marine sediments.

As shown in Figs. 3c and 3d, there are weak negative correlations of K_2O and Rb with SiO_2 for marine sediments (γ = –0.78 and –0.69, respectively). Significantly, most of the Sanbagawa samples show K, Si and Rb compositions overlapping those of marine sediments along Japan Arc. According to Plank and Langmuir (1998), K in clastic detritus is diluted by biogenic silica. However, a weak negative correlation is found for marine sediments in the SiO_2–K_2O diagram, whereas scattered nature is shown by the Sanbagawa samples. This suggests that components other than clastic detritus and biogenic silica are contributing to the Sanbagawa samples. Different degrees of diagenetic K and Rb uptake by clay minerals and variations in detrital clay mineralogy (e.g., illite vs. kaolinite) are considered as an additional cause of K and Rb variations.

The Rb/K_2O ratios in all metamorphic grades of the Sanbagawa samples fall within the range recorded for marine sediments apart from two outliers (Fig. 4). This correlation suggests that K_2O and Rb abundances of the Sanbagawa samples are modified by the diagenetic uptake perhaps controlled by clay mineralogy (K, Rb-rich illite vs. -poor kaolinite).

We conclude that all metamorphic grades of the samples (chlorite ~ oligoclase–biotite zone) experienced insignificant dissolution of Si, Ti, Al, K and Rb during prograde metamorphism in bulk, although local re-distribution of K and Rb is feasible.

Chemical changes in the Sanbagawa pelitic schists during prograde metamorphism

In order to identify chemical changes in the Sanbagawa pelitic schists during prograde metamorphism, selected elements have been plotted against horizontal distance from the northernmost sample (Fig. 5).

Arsenic dissolution As shown in Fig. 5a, most chlorite zone samples and some garnet zone samples have relatively high As contents (6~10 ppm), while other samples in the higher metamorphic grade have As contents below the detection limit: less than 0.1 ppm. In addition, the garnet zone samples with higher As contents (Nos. 10 and 11) occur up until upper garnet zone close to the iso-grade between the chlorite and garnet zones (Figs. 1b and 5a). It is highly probable that As dissolution was enhanced significantly during upper–garnet zone metamorphism (P ~ 0.75 GPa, T ~ 450°C).

Some marine sediments show lower As contents, which can be caused by (i) higher contribution of biogenic silica with low As content and (ii) lower contribution of Fe–Mn oxyhydroxides with high As concentration (Maher, 1984). Such marine sediments with lower As contents may be the source for two chlorite zone samples with low As contents (Nos. 2 and 4: 2.35 and 2.66 ppm, respectively). These samples are characterized by (i) higher SiO_2 contents (>70 wt%) and (ii) lower Fe_2O_3 and MnO contents (<3.2 wt% and <0.07 wt%, respectively) relative to other chlorite zone samples (Table 2). The former probably means higher contribution of biogenic silica, and the latter suggests lower contribution of Fe–Mn oxyhydroxides.

Graphitization of kerogens The H/C, O/C and N/C ratios of kerogens extracted from the Sanbagawa samples de-

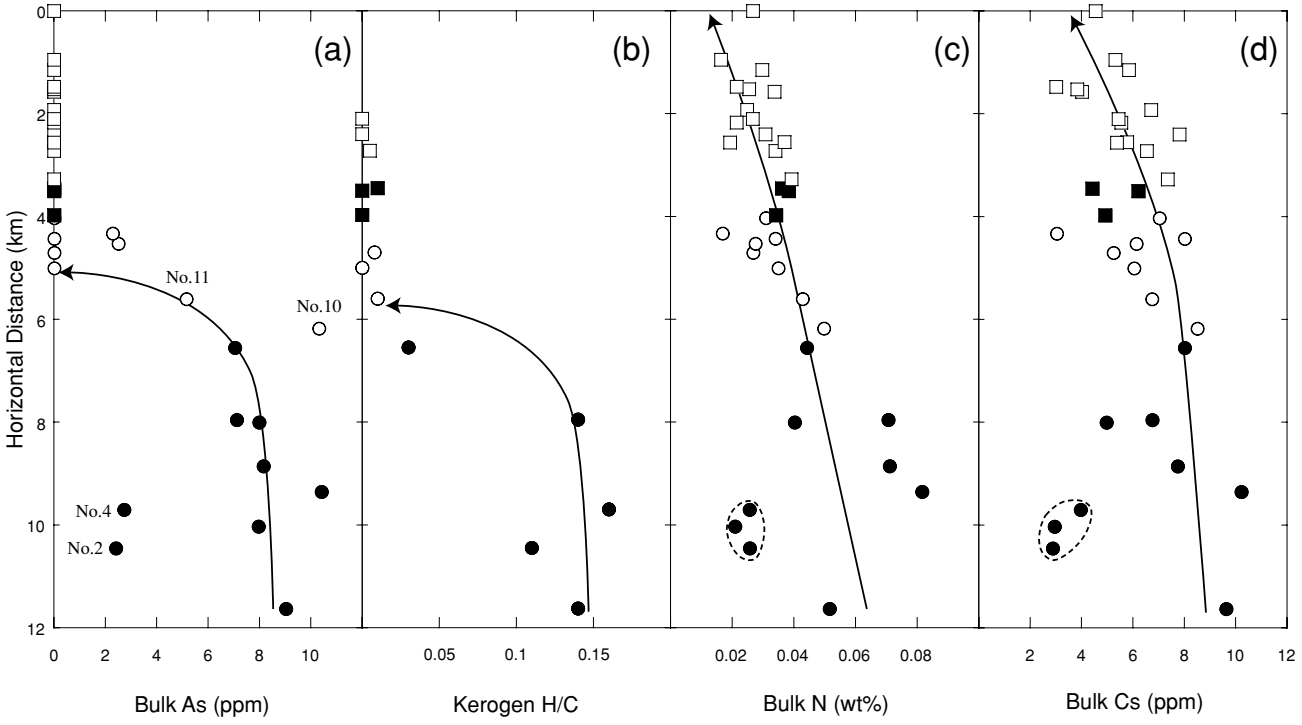

Fig. 5. Variations of (a) bulk As content, (b) kerogen H/C ratio, (c) bulk N content and (d) bulk Cs content against metamorphic grade of the Sanbagawa pelitic schists. The vertical axis represents horizontal distance of each sampling site from that of the northernmost sample that belongs to the highest metamorphic grade. Sample symbols are closed circle: chlorite zone sample, open circles: garnet zone, closed square: albite–biotite zone, and open square: oligoclase–biotite zone.

crease dramatically near the iso-grad between the chlorite and garnet zones and remain close to zero from the upper–garnet through the oligoclase–biotite zones (Table 3; Fig. 5b). Apparent d_{002} and peak width (FWMH) also show a similar decrease and reach the value of ordered graphite (d_{002} = 3.33~3.36). Hence, it is suggested that the graphitization proceeded with release of CH_4, CO_2 and/or H_2O during prograde metamorphism from the upper–chlorite to lower–garnet zones. Arsenic contents sharply decrease at the same point where the process of graphitization is complete (Fig. 5a).

NH_4^+ dissolution As shown in Fig. 5c, N contents of the Sanbagawa samples decrease successively from the chlorite to the oligoclase–biotite zones, except for three low N samples from the chlorite zone. As stated earlier, two samples (Nos. 2 and 4) among these three show higher SiO_2 content and may be diluted with the biogenic component. Bebout and Fogel (1992) compared N/K_2O ratios among the Catalina meta-sedimentary rocks in order to examine NH_4^+ dissolution from subducting sediments into fluids, supposing that most of nitrogen exists as NH_4^+ substituting for K^+ (Stevenson, 1962; Honma and Itihara, 1981). Nitrogen is also likely to be contained in organic matters. However, in the case of the Sanbagawa samples, the nitrogen content of kerogens is estimated to be low relative to that of bulk rock (Table 4), which indicates that most of nitrogen exists as NH_4^+.

A decrease in N/K_2O ratios with increasing metamorphic grade (Fig. 6a) clearly suggests NH_4^+ (N) dissolution from the Sanbagawa samples is likely to have occurred successively during prograde metamorphism from the chlorite to oligoclase–biotite zones. In particular, it was probably enhanced during prograde metamorphism from the chlorite to garnet zones ($P \sim 0.7$ GPa, $T \sim 400$°C) and from the albite–biotite to oligoclase–biotite zones ($P \sim 0.9$ GPa, $T \sim 550$°C), according to significant differences in N/K_2O ratios between the chlorite and garnet zone samples and the albite–biotite and oligoclase–biotite zone samples, respectively. The N/K_2O ratios are not constant among the samples in the same metamorphic grade. This may be due to (i) inconstant N/K_2O ratios of marine sediments, (ii) local redistribution of K in diagenetic process, and (iii) variable degree of the NH_4^+ dissolution among the samples. Regarding (i), Müller (1977) reported that NH_4^+/K_2O ratios of marine sediments are dependent on their sedimentological or stratigraphical unit. Rests are deduced from the observations of the Sanbagawa samples.

Cesium dissolution A slight decrease in Cs contents is observed with increasing metamorphic grade, though Cs

Table 3. Chemical compositions and X-ray diffraction data of kerogens, and bulk arsenic contents of the Sanbagawa pelitic schists. The order of samples corresponds to the increasing order of metamorphic grade from south to north along the Asemi river.

Sample No.	Metamorphic zone	C	N	H	O	Total	H/C	O/C	N/C	FWMH	Apparent	Bulk As
		(wt%)					(atom)			(deg)	d_{002} (A)	(ppm)
1		72.5	0.20	0.86	2.3	75.8	0.14	0.023	0.002	n.d.	3.49	8.59
2		63.1	0.17	0.60	2.6	66.5	0.11	0.031	0.002	n.d.	n.d.	2.35
4	Chlorite Zone	77.4	0.25	1.03	2.9	81.6	0.16	0.028	0.003	4.00	n.d.	2.66
8		77.5	0.27	0.89	2.2	80.08	0.14	0.021	0.003	n.d.	n.d.	6.86
9		80.6	0.10	0.22	0.8	81.6	0.03	0.007	0.001	1.85	3.42	6.70
11	Garnet Zone	74.6	n.d.	0.08	0.9	83.7	0.01	0.009	—	1.36	3.39	4.94
12		88.1	n.d.	n.d.	0.3	88.4	—	0.003	—	0.51	3.34	n.d.
13		93.4	0.06	0.07	0.7	94.2	0.008	0.006	0.001	0.53	3.35	n.d.
18	Albite–biotite Zone	83.2	n.d.	n.d.	0.5	83.7	—	0.005	—	0.44	3.32	n.d.
20		92.4	n.d.	n.d.	0.9	93.3	—	0.007	—	0.43	3.36	n.d.
21		75.6	n.d.	0.07	1.7	77.3	0.01	0.017	—	0.56	3.32	n.d.
22	Oligoclase–biotiteZone	82.7	n.d.	0.04	1.5	84.2	0.005	0.014	—	0.31	3.36	n.d.
24		88.0	n.d.	n.d.	0.3	88.3	—	0.003	—	0.44	3.32	n.d.
28		87.9	n.d.	n.d.	0.5	88.4	—	0.004	—	0.43	3.35	n.d.

Note: "n.d." of X-ray diffraction data (FWHM and Apparent d_{002}) means not detected because of unclear graphite peaks in X-ray diffraction analysis.
"n.d." of other data means not detected because of under detection limit.

concentration of the Sanbagawa samples is variable in each metamorphic grade (Fig. 5d). As shown in Fig. 6b, some samples from higher metamorphic grades—the albite–biotite and oligoclase–biotite zones—have lower Cs/Rb ratios than low grade metamorphic samples. These results show possible dissolution of Cs into fluids was probably enhanced during prograde metamorphism from the garnet to albite–biotite zones ($P \sim 0.8$ GPa, $T \sim 500$°C). The proportion of the Cs loss is estimated to have been 0% to 40% by the change in Cs/Rb ratios (Fig. 6b). Nine samples out of 17 in the albite–biotite and oligoclase–biotite zones have lower Cs/Rb ratio than in low metamorphic grade samples. All but one sample show <40% Cs dissolution. The major Cs dissolution is apparent between garnet and albite–biotite zones.

Mechanisms of the element dissolution

Possible sources of free fluid during prograde metamorphism The major discussion is about the sources of free fluids dissolving As, Cs and NH_4^+. The candidates for the fluid source are meta-sedimentary rocks, meta-mafic rocks and meta-ultramafic rocks that may flush over meta-sedimentary rocks (e.g., Bebout *et al*., 2007).

Meta-sedimentary rocks themselves might have released fluids successively during prograde metamorphism from the chlorite to albite–biotite zones, because breakdown of chlorite ($2\text{Chlorite} + 4\text{Qtz} = 3\text{Garnet} + 8H_2O$) continued from the chlorite to garnet zones and reaction of chlorite with phengite ($\text{Chlorite} + 2\text{phengite} = \text{muscovite} + \text{biotite} + \text{Qtz} + 4H_2O$) continued from the garnet to albite–biotite zones (Sakai *et al*., 1985; Inui and Toriumi, 2002; Hacker, 2008).

Meta-mafic rocks decrease their maximum H_2O content from 3.4 wt% to 2.3 wt% from greenschist to epidote–amphibolite facies, i.e., from garnet to oligoclase–biotite zones (Peacock, 1993; Hacker, 2008). In this context, meta-mafic rocks could release fluids during prograde metamorphism from the garnet to albite–biotite zones, if source mafic rocks contained H_2O content larger than 2.3 wt% due to hydrothermal alteration before subduction. On the contrary, meta-ultramafic rocks cannot have produced fluids due to antigorite breakdown at 600°C during prograde metamorphism of the overlying meta-sedimentary rocks from the chlorite to albite–biotite zones (peak T: up to 600°C). That's because conduction of heat downward from mantle wedge into the top of slab results in warmer P-T path for the top of slab compared to the base (Peacock, 1990; Hacker, 2008).

Mechanism of the As dissolution Dramatic As dissolution was observed in the Sanbagawa samples during upper–garnet zone metamorphism ($P \sim 0.75$ GPa, $T \sim 450$°C). Such As dissolution is also experienced by the Catalina samples only during the higher-T prograde metamorphism reaching up to epidote–blueschist/amphibolite or amphibolite facies (Bebout *et al*., 1999). Therefore it occurred at about 400~450°C both in the Catalina and

Table 4. Estimated ratios of nitrogen in kerogens against bulk amounts of nitrogen of the Sanbagawa pelitic schists. On the supposition that all carbon in the schists is derived from kerogens, the ratios are calculated as below;

$$\frac{Bulk\ \ Carbon\ \ [ppm]}{Bulk\ \ Nitrogen\ \ [ppm]} \times \frac{Nitrogen\ \ Content\ \ of\ \ Kerogen\ \ [wt\%]}{Carbon\ \ Content\ \ of\ \ Kerogen\ \ [wt\%]} \times 100$$

Sample No.	Metamorphic zone	Kerogen		Bulk rock		Estimated ratio (%)
		C (wt%)	N (wt%)	C (ppm)	N (ppm)	
1	Chlorite Zone	72.5	0.20	3,300	490	1.9
2		63.1	0.17	2,000	250	2.2
4		77.4	0.25	1,500	250	1.9
8		77.5	0.27	6,100	680	3.1
9		80.6	0.10	5,200	420	1.5
11	Garnet Zone	74.6	0.07	2,900	410	0.7
12		88.1	n.d.	3,700	340	—
13		93.4	0.06	1,900	260	0.5
18	Albite–biotite Zone	83.2	n.d.	1,100	330	—
20		92.4	n.d.	2,800	350	—
21	Oligoclase–biotite Zone	75.6	n.d.	5,000	380	—
22		82.7	n.d.	2,600	330	—
24		88.0	n.d.	2,500	360	—
28		87.9	n.d.	5,400	240	—

Note: "n.d." means not detected because of under detection limit.

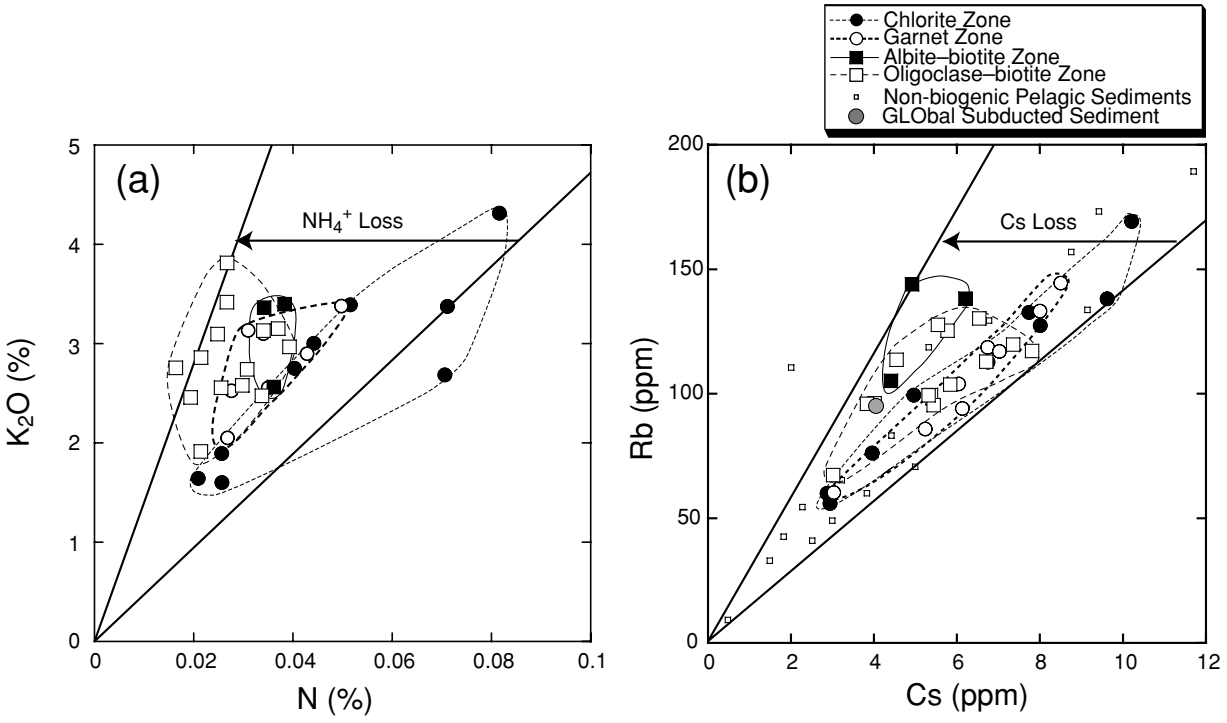

Fig. 6. Relationship diagrams of (a) N–K_2O and (b) Cs–Rb. Sample symbols are the same as those in Fig. 5. Non-biogenic marine sediments from world-wide ocean (Ben Othman et al., 1989) and GLOSS (global subducted sediment) by Plank and Langmuir (1998) are also plotted by small open squares and gray large circle, respectively.

Sanbagawa samples. Interestingly, the As dissolution was enhanced along with completion of graphitization during prograde metamorphism in both of the samples (Bebout *et al*., 1999). Also, previous studies pointed out that ordered graphite in metamorphic rocks is attained at 400~500°C with little pressure dependence (Landis, 1971; Wang, 1989). From the above overview, we suggest that As dissolution from meta-sedimentary rocks may possibly be associated with graphitization of kerogens, although the mechanism is not clear in detail.

Mechanism of the NH_4^+ dissolution As mentioned above, NH_4^+ dissolution from the Sanbagawa samples is likely to have occurred successively during prograde metamorphism from the chlorite to oligoclase–biotite zones. At these metamorphic stages, meta-sedimentary rocks could release fluids successively. It is, therefore, probable to consider that fluids responsible for NH_4^+ dissolution was supplied from meta-sedimentary rocks themselves.

In the present Sanbagawa samples the major potassium-bearing mineral is phengitic muscovite, and both of NH_4^+ and Rb^+ are likely to exist in XII sites. There is a subtle difference of ionic radii between Rb^+ (1.72 Å from Shannon, 1976) and NH_4^+ (1.67 to 1.72 Å from Knop *et al*., 1979), suggesting that Rb and NH_4^+ should dissolve from muscovite into fluids in nearly the same proportions. However, the Sanbagawa samples experienced only NH_4^+ dissolution but not Rb dissolution. This indicates that the NH_4^+ dissolution was caused by fluids with a high potential to dissolve NH_4^+ preferentially; for example, fluids containing high concentration of metal elements that form a stable complex with NH_4^+.

Another possible explanation of the preferential NH_4^+ dissolution in the Sanbagawa samples is oxidation of NH_4^+ to soluble NO_2^- or NO_3^-. According to Mottl *et al*. (2004), sulfate contents of brines from top of Mariana forearc seamounts increase with increasing distance from the trench axis, reaching a concentration nearly twice that in seawater at Conical Seamount at 90 km distance from the trench axis. This observation suggests that the dehydrated fluid from shallow subduction zone, comparable depth range to the Sanbagawa samples, may have an oxidative character. If so, such the fluid can oxidize NH_4^+ to soluble oxide forms.

Mechanism of the Cs dissolution As mentioned before, the Cs dissolution from the Sanbagawa samples into fluids was probably enhanced during prograde metamorphism from the garnet to albite–biotite zones (P ~ 0.8 GPa, T ~ 500°C).

At the metamorphic condition from the garnet to albite–biotite zones, maximum H_2O content of meta-mafic rocks decreases from 3.4 w% to 2.3 wt% and excess H_2O in meta-mafic rocks was released. External fluids from meta-mafic rocks to the meta-sedimentary rocks are the another candidate for the source of fluids dissolving Cs.

As shown in Figs. 5d and 6b, various degree of the Cs dissolution is observed in the same metamorphic grade. External flow of fluids rising from subducting slab to mantle wedge is recognized as "channelized flow" (Miller *et al*., 2003; Zack and John, 2007; John *et al*., 2004, 2008). Some models suggest that the channelized flow, gathering fluid-filled micro-cracks, has enough high pressure for opening fractures allowing the flow to rise up inside slab with low permeability due to high-pressure (Davies, 1999; Miller *et al*., 2003). The characteristics of the channelized flow can explain various degrees of the Cs dissolution (Figs. 5d and 6b). Zack and John (2007) pointed out that the channelized flow is heterogenous and yields closed system behavior in some parts of slabs. This probably resulted in heterogenous degrees of the Cs dissolution.

Moreover, possible factors that may control element mobility in subduction zones have been identified. There are thermal history of the slab (Bebout *et al*., 1999), and open or closed behaviors of the fluids in the slab (John *et al*., 2004, 2008). Studies of meta-sedimentary rocks formed in various subduction zones are necessary to investigate the details of the element dissolution processes. However, we could not discuss these factors in detail because of lack of enough data.

Comparison with other meta-sedimentary rocks

We will examine whether the suggested dissolution mechanisms in this study can be applicable to other meta-sedimentary rocks. We refer to other studies comparable to the present in which meta-sedimentary rocks are analyzed to elucidate the element mobility: the Catalina schists in California (e.g., Bebout and Fogel, 1992; Bebout *et al*., 1999) and Schists Lustrés nappe in western Alps, Europe (Busigny *et al*., 2003). The former show a variety of temperature condition, while the latter show relatively low temperature condition in their *P-T* path during subduction. Therefore it is possible to make sure whether the difference of depths where both meta-mafic rocks and meta-sedimentary rocks release fluids, i.e., thermal characteristics of the slab can control the dissolution of Cs and NH_4^+ from meta-sedimentary rocks into fluids.

The Catalina meta-sedimentary rocks Bebout *et al*. (1999, 2007) suggested that Cs dissolution from the Catalina meta-sedimentary rocks was enhanced only during the higher-T prograde metamorphism (up to epidote–blueschist/amphibolite or amphibolite facies), while the dissolution was not enhanced during the lower-T one (lawsonite–albite ~ lawsonite–blueschist facies), comparing Cs/Rb ratios among the samples. According to Peacock (1993), maximum H_2O contents of meta-mafic rocks decrease during the higher-T prograde metamorphism (greenschist ~ epidote–blueschist/amphibolite or amphibolite facies), while it doesn't decrease during

lower-*T* one (lawsonite–albite ~ lawsonite–blueschist facies). Therefore, the Cs dissolution from the higher-*T* Catalina samples is considered to have been caused by dehydration of the underlying meta-mafic rocks along higher-*T P-T* path. This view is consistent with Bebout *et al*. (2007) and Zack *et al*. (2001), who suggested external fluid flow is required for the Cs dissolution from the Catalina samples. Significantly, the degree of the Cs dissolution is different between the Catalina and Sanbagawa samples; ~75% Cs was dissolved from the former (Bebout *et al*., 1999), while ~40% Cs from the latter. One of the reason for such a difference is thought to be variation in propagation of the channelized flow such as a difference in initial H_2O content of mafic rocks.

The NH_4^+ dissolution from the Catalina meta-sedimentary rocks was associated with successive dehydration of the meta-sedimentary rocks with increasing metamorphic grade (Bebout and Fogel, 1992). On the other hand, Rb dissolution from the Catalina samples is not confirmed (Bebout *et al*., 1999). These results are similar to the Sanbagawa samples. Therefore it is possible that the NH_4^+ dissolution from the Catalina samples was caused by fluid release from the meta-sedimentary rocks alone. Furthermore, Bebout (1997) indicated that N isotopic compositions in the Catalina samples are controlled by local scale of fluids-rock interactions. This result may mean that NH_4^+ was dissolved into local fluids derived from the Catalina meta-sedimentary rocks themselves.

Schists Lustrés nappe Busigny *et al*. (2003) analyzed meta-sedimentary rocks of the Schists Lustrés nappe, which experienced low-*T P-T* path reaching up to UHP (ultra-high-pressure) facies (peak *P*: 2.9 GPa, peak *T*: 630°C) in cool subduction zone. They demonstrated that insignificant amount of Cs was dissolved from the samples during prograde metamorphism up to UHP facies because Cs/Rb ratios of all samples are comparable to unmetamorphosed sedimentary protoliths. Significantly, Busigny *et al*. (2003) also pointed out that the samples behaved as a closed system on the basis of the isotopic ratios of C and O in calcite. This implies undeveloped fluids in the Schists Lustrés nappe samples in contrast to the Sanbagawa and Catalina (additional external fluid perhaps from meta-mafic unit). Such a closed element behavior was possibly caused by (i) insufficient element dissolution from meta-mafic rocks due to low-*T* path and/or (ii) impermeable fluid behavior in the Schists Lustrés nappe unit under high pressure, and (iii) less external fluid supplied to the meta-sediment body.

Conclusions

We discussed element dissolution from the Sanbagawa schists into fluids during prograde metamorphism from the chlorite to oligoclase–biotite zones by means of their chemical compositions.

(i) Insignificant dissolution of major elements (Si, Ti, Al and K) and Rb occurred.

(ii) Dramatic As dissolution occurred during the upper–garnet zone metamorphism (*P*: about 0.8 GPa, *T*: about 450°C). It accompanied formation of ordered graphite.

(iii) NH_4^+ dissolution was enhanced successively during prograde metamorphism from the chlorite to oligoclase–biotite zones. This dissolution was caused by dehydration of the pelitic schists, which produced fluids with a high potential to dissolve or oxide NH_4^+.

(iv) Cs dissolution was enhanced during prograde metamorphism from the garnet to albite–biotite zones. The degree of Cs dissolution, however, is heterogeneous in the same metamorphic grade. This dissolution may be attributed to effective fluid transfer by the channelized flow from the underlying meta-mafic rocks, although other factors such as chemical composition of fluids must also be discussed.

In this study, we elucidated the element dissolution processes from subducting sediments into fluids at shallow depths (up to oligoclase–biotite zone) and the factors controlling the element mobility. This study also indicates that chemical changes in meta-sedimentary rocks with increasing metamorphic grade are an effective way for examination of element dissolution processes in subduction zones.

Acknowledgments—We thank Dr. M. Enami for geological advices and discussions. K. Hattori is also appreciated for discussing our data and introducing useful papers. We are also grateful to Dr. S. R. Wallis for giving helpful comments for this paper. Critical comments from Dr. Gen Shimoda, National Institute of Industrial Science and Technology, Japan, and an anonymous reviewer significantly improved the manuscript.

References

Banno, S. and Sakai, C. (1989) Geology and metamorphic evolution of the Sanbagawa metamorphic belt, Japan. *Evolution of Metamorphic Belts, Geol. Soc. Spec. Publ.*, No. 43 (Daly, J. S., Cliff, R. A. and Yardley, B. W. D., eds.), 519–532.

Banno, S., Higashino, T., Otsuki, M., Itaya, T. and Nakajima, T. (1978) Thermal structure of the Sanbagawa metamorphic belt in central Shikoku. *J. Phys. Earth* **26** (Suppl.), 345–356.

Bebout, G. E. (1995) The impact of subduction-zone metamorphism on mantle-ocean chemical recycling. *Chem. Geol.* **126**, 191–218.

Bebout, G. E. (1997) Nitrogen isotope tracers of high-temperature fluid-rock interactions: Case study of the Catalina Schist, California. *Earth Planet. Sci. Lett.* **151**, 77–90.

Bebout, G. E. and Fogel, M. L. (1992) Nitrogen-isotope compositions of metasedimentary rocks in the Catalina Schist, California: Implications for metamorphic devolatilization

history. *Geochim. Cosmochim. Acta* **56**, 2839–2849.
Bebout, G. E., Ryan, J. G., Leeman, W. P. and Bebout, A. E. (1999) Fractionation of trace elements by subduction-zone metamorphism—effect of convergent-margin thermal evolution. *Earth Planet. Sci. Lett.* **171**, 63–81.
Bebout, G. E., Bebout, A. E. and Graham, C. M. (2007) Cycling of B, Li, and LILE (K, Cs, Rb, Ba, Sr) into subduction zones: SIMS evidence from micas in high-*P*/*T* metasedimentary rocks. *Chem. Geol.* **239**, 284–304.
Ben Othman, D., White, W. M. and Patchett, J. (1989) The geochemistry of marine sediments, island arc magma genesis, and crust-mantle recycling. *Earth Planet. Sci. Lett.* **94**, 1–21.
Busigny, V., Cartigny, P., Philippot, P., Ader, M. and Javoy, M. (2003) Massive recycling of nitrogen and other fluid-mobile elements (K, Rb, Cs, H) in a cold slab environment: evidence from HP to UHP oceanic metasediments of the Schistes Lustrés nappe (western Alps, Europe). *Earth Planet. Sci. Lett.* **215**, 27–42.
Davies, J. H. (1999) The role of hydraulic fractures and intermediate-depth earthquakes in generating subduction-zone magmatism. *Nature* **398**, 142–145.
Enami, M. (1982) Oligoclase–biotite zone of the Sanbagawa metamorphic terrain in the Bessi district, central Shikoku, Japan. *Chishitu-gaku Zasshi* **88**, 887–900.
Enami, M., Wallis, S. R. and Banno, Y. (1994) Paragenesis of sodic pyroxene-bearing quartz schists: implications for the *P-T* history of the Sanbagawa belt. *Contrib. Mineral. Petrol.* **116**, 182–198.
Hacker, B. R. (2008) H_2O subduction beyond arcs. *Geochem. Geophys. Geosyst.* **9**, 24, Q03001, doi:10.1029/2007GC001701.
Hattori, K. H. and Guillot, S. (2003) Volcanic fronts from as a consequence of serpentinite dehydration in the forearc mantle wedge. *Geoogy* **31**, 525–528.
Higashino, T. (1990) The higher grade metamorphic zonation of the Sambagawa metamorphic belt in central Shikoku, Japan. *J. Metamor. Geol.* **8**, 413–423.
Honma, H. and Itihara, Y. (1981) Distribution of ammonium in minerals of metamorphic and granitic rocks. *Geochim. Cosmochim. Acta* **45**, 983–988.
Inui, M. and Toriumi, M. (2002) Prograde pressure-temperature paths in the pelitic schists of the Sambagawa metamorphic belt, SW Japan. *J. Metamor. Geol.* **20**, 563–580
Isozaki, Y. and Itaya, T. (1990) Chronology of Sanbagawa metamorphism. *J. Metamor. Geol.* **8**, 401–411.
John, T., Scherer, E. E., Haase, K. and Schenk, V. (2004) Trace element fractionation during fluid-induced eclogitization in a subducting slab: trace element and Lu–Hf–Sm–Nd isotope systematics. *Earth Planet. Sci. Lett.* **227**, 441–456.
John, T., Klemd, R., Gao, J. and Garbe-Schönberg, C. (2008) Trace-element mobilization in slabs due to non steady-state fluid-rock interaction: Constraints from an eclogite-facies transport vein in blueschist (Tianshan, China). *Lithos* **103**, 1–24.
Johnson, M. C. and Plank, T. (1999) Dehydration and melting experiments constrain the fate of subducted sediments. *Geochem. Geophys. Geosyst.* **1**, 1007, doi:10.1029/1999GC000014.
Knop, O., Oxton, I. A. and Falk, M. (1979) Infrared spectra of the ammonium ion in crystals. Part VI. Hydrogen bonding in simple and complex ammonium halides. *Can. J. Chem.* **57**, 404–423.
Kogiso, T., Tatsumi, Y. and Nakano, S. (1997) Trace element trasport during dehydration processes in the subducted oceanic crust: 1. Experiments and implications for the origin of ocean island basalt. *Earth Planet. Sci. Lett.* **148**, 193–205.
Landis, C. A. (1971) Graphitization of dispersed carbonaceous material in metamorphic rocks. *Contrib. Mineral. Petrol.* **30**, 34–45.
Leeman, W. P. (1996) Boron and other fluid-mobile elements in volcanic arc lavas: Implications for subduction processes. *Subduction: Top to Bottom, Amer. Geophys. Union, Geophs. Monogr.* **96** (Bebout, G. E., Scholl, D. W., Kirby, S. H. and Platt, J. P., eds.), 269–276.
Maher, W. A. (1984) Mode of occurrence and speciation of arsenic in some pelagic and estuarine sediments. *Chem. Geol.* **47**, 333–345.
McCulloch, M. T. and Gamble, J. A. (1991) Geochemical and geodynamical constrains on subduction zone magmatism. *Earth Planet. Sci. Lett.* **102**, 358–374.
Miller, S. A., Van der Zee, W., Olgaard, D. L. and Connolly, J. A. D. (2003) A fluid-pressure feedback model of dehydration reactions: experiments, modelling, and application to subduction zones. *Tectonophysics* **370**, 241–251.
Mottl, M. J., Wheat, C. G., Fryer, P., Gharib, J. and Martin, J. B. (2004) Chemistry of springs across the Mariana forearc shows progressive devolatilization of the subducting plate. *Geochim. Cosmochim. Acta* **68**, 4915–4933.
Müller, P. J. (1977) C/N ratios in Pacific deep-sea sediments: Effect of inorganic ammonium and organic nitrogen compounds sorbed by clays. *Geochim. Cosmochim. Acta* **41**, 765–776.
Nakano, T. and Nakamura, E. (2001) Boron isotope geochemistry of metasedimentary rocks and tourmalines in a subduction zone metamorphic suite. *Phys. Earth Planet. Inter.* **127**, 233–252.
Peacock, S. M. (1990) Fluid processes in subduction zones. *Science* **248**, 329–336.
Peacock, S. M. (1993) The importance of blueschist → eclogite dehydration reactions in subducting oceanic crust. *Geol. Soc. Amer. Bull.* **105**, 684–694.
Perfit, M. R., Gust, D. A., Bence, A. E., Arculus, R. J. and Taylor, S. R. (1980) Chemical characteristics of island-arc basalts: implication for mantle sources. *Chem. Geol.* **30**, 227–256.
Plank, T. and Langmuir, C. H. (1993) Tracing trace elements from sediment input to volcanic output at subduction zones. *Nature* **362**, 739–743.
Plank, T. and Langmuir, C. H. (1998) The chemical composition of subducting sediment and its consequences for the crust and mantle. *Chem. Geol.* **145**, 325–394.
Sakai, C., Banno, S., Toriumi, M. and Higashino, T. (1985) Growth history of garnet in pelitic schists of the Sanbagawa metamorphic terrain in central Shikoku. *Lithos* **18**, 81–95.
Shannon, R. D. (1976) Revised effective Ionic Radii and systematic studies of interatomic distances in halides and chalcogenides. *Acta Crystallogr.* **A32**, 751–767.

Spandler, C., Hermann, J., Arculus, R. and Mavrogenes, J. (2003) Redistribution of trace elements during prograde metamorphism from lawsonite blueschist to eclogite facies; implications for deep subduction-zone processes. *Contrib. Mineral. Petrol.* **146**, 205–222.

Spandler, C., Hermann, J., Arculus, R. and Mavrogenes, J. (2004) Geochemical heterogeneity and element mobility in deeply subducted oceanic crust; insights from high-pressure mafic rocks from New Caledonia. *Chem. Geol.* **206**, 21–42.

Spandler, C., Mavrogenes, J. and Hermann, J. (2007) Experimental constrains on element mobility from subducted sediments using high-*P* synthetic fluid/melt inclusions. *Chem. Geol.* **239**, 228–249.

Stevenson, F. J. (1962) Chemical state of the nitrogen in rocks. *Geochim. Cosmochim. Acta* **26**, 797–809.

Sugisaki, R. (1978) Chemical composition of argillaceous sediments on the Pacific margin of Southwest Japan. *Geol. Survey of Japan, Cruise Report* **9**, 65–73.

Sugisaki, R. (1981) Major-element chemistry of bottom sediments from the GH79-1 area, the northern central Pacific basin. *Geol. Survey of Japan, Cruise Report* **15**, 236–244.

Sugisaki, R. and Yamamoto, K. (1984) Major element chemistry of pacific marine sediments around 10°N and 170°W: samples for GH80-5 cruise, Geological Survey of Japan. *Geol. Survey of Japan Cruise Report* **20**, 198–214.

Takasu, A. (1989) *P-T* histories of peridotite and amphibolite tectonic blocks in the Sanbagawa metamorphic belt, Japan. *The Evolution of Metamorphic Belts* (Daly, J. S., Cliff, R. A. and Yardley, B. W. D., eds.), 533–538, Blackwell Scientific Publications, Oxford.

Tatsumi, Y., Hamilton, D. L. and Nesbitt, R. W. (1986) Chemical characteristics of fluid phase released from a subducted lithosphere and origin of arc magmas: Evidence from high-pressure experiments and natural rocks. *J. Volcanol. Geotherm. Res.* **29**, 293–309.

Tera, F., Brown, L., Morris, J., Selwyn, I., Sacks, I. S., Klein, J. and Middleton, R. (1986) Sediment incorporation in island-arc magmas: Inferences from ^{10}Be. *Geochim. Cosmochim. Acta* **50**, 535–550.

Wallis, S. R. (1998) Exhuming the Sanbagawa metamorphic belt: the importance of tectonic discontinuities. *J. Metamor. Geol.* **16**, 83–95.

Wallis, S. R. and Aoya, M. (2000) A re-evaluation of eclogite facies metamorphism in SW Japan: proposal for an eclogite nappe. *J. Metamor. Geol.* **18**, 653–664.

Wallis, S., Takasu, A., Enami, M. and Tsujimori, T. (2000) Eclogite and Related Metamorphism in the Sanbagawa Belt, Southwest Japan. *Bull. Res. Inst. Nat. Sci., Okayama Univ. of Sci.* **26**, 3–17.

Wang, G.-F. (1989) Carbonaceous material in the Ryoke metamorphic rocks, Kinki district, Japan. *Lithos* **22**, 305–316.

White, W. M. and Dupré, B. (1985) Isotope and trace element geochemistry of sediments from the Barbados Ridge–Demerara Plain region, Atlantic Ocean. *Geochim. Cosmochim. Acta* **49**, 1875–1886.

You, C. F., Castillo, P. R., Gieskes, J. M., Chan, L. H. and Spivack, A. J. (1996) Trace element behavior in hydrothermal experiments: Implications for fluid processes at shallow depths in subduction zones. *Earth Planet. Sci. Lett.* **140**, 41–52.

Zack, T. and John, T. (2007) An evaluation of reactive fluid flow and trace element mobility in subducting slabs. *Chem. Geol.* **239**, 199–216.

Zack, T., Rivers, T. and Foley, S. F. (2001) Cs–Rb–Ba systematics in phengite and amphibole: an assessment of fluid mobility at 2.0 GPa in eclogites from Trescolmen, Central Alps. *Contrib. Mineral. Petrol.* **140**, 651–669.